

Tomographic methods for universal estimation in quantum optics

GIACOMO MAURO D'ARIANO

Quantum Optics & Information Group,

Istituto Nazionale di Fisica della Materia, Unità di Pavia

Dipartimento di Fisica "A. Volta", via Bassi 6, I-27100 Pavia, Italy

Summary. — "Quantum Tomography" is a general method for estimating arbitrary ensemble averages—including the density matrix itself— of any quantum system, through the measurement of a "quorum" of observables. Recently the method has been extended to the estimation of the matrix form of any "quantum operation" (i. e. quantum evolutions and measurements), using only a fixed "entangled state" as the input state, the entangled state playing the role of all possible input states in "quantum parallel". A short review of the theory is presented, with a list of examples of applications for different quantum systems, and with particular focus on quantum optics. Some results from experiments in quantum optics are reexamined. Hints and perspectives on future developments are given at the end of the paper.

1. – Introduction

The possibility of "measuring the quantum state" has puzzled physicists in the last half century, since the earlier theoretical studies of Fano [1]. W. Pauli [2] in a footnote of the *Encyclopedia of Physics* wrote: "The mathematical problem, as to whether for given functions $W(\vec{x})$ and $W(\vec{p})$, the wave function ψ , if such function exists, is always uniquely

determined, has still not been investigated in all its generality” [by $W(\vec{x})$ and $W(\vec{p})$ Pauli denoted the probability distributions of position and momentum of a particle, respectively, whereas, for “if such function exists” he meant if $W(\vec{x})$ and $W(\vec{p})$ are compatible]. The answer to Pauli’s question was clearly negative, since the probabilities $W(\vec{x})$ and $W(\vec{p})$ alone cannot determine the correlation between position and momentum, which could be obtained, for example, from a *joint* measurement of \vec{x} and \vec{p} . However, a joint measurement of two conjugated observables would exhibit an additional noise equivalent to an effective quantum efficiency $\eta = 1/2$ [3], and as we will see in Subsect. 3’6, this is exactly the threshold below which the density matrix cannot be measured.

That more than two observables—actually a complete set of them—are needed for a complete determination of the density matrix was clear from the work of Fano [1], and it is explicitly remarked in the book of d’Espagnat [4]. However, since it is difficult to devise concretely measurable observables—other than position, momentum and energy⁽¹⁾—such a fundamental problem—measuring the quantum state!—has remained at the level of mere speculation for many years. The issue finally entered the realm of experiments only less than ten years ago, after the pioneering experiments by Raymer’s group [6], in the domain of quantum optics.

What is so special with quantum optics? In quantum optics, differently from quantum mechanics of particles, there is the unique opportunity of measuring all possible linear combinations of position Q and momentum P of a harmonic oscillator, which is represented by a single mode of the electromagnetic field. As explained in Subsect. 3’1, such measurement can be achieved by means of a balanced homodyne detector, which measures the quadrature $X_\phi = \frac{1}{2}(a^\dagger e^{i\phi} + a e^{-i\phi})$ of a field mode at any desired phase ϕ with respect to the local oscillator (LO) [as usual a denotes the annihilator of the field mode]. The first technique to reconstruct the density matrix from homodyne measurements—so called *homodyne tomography*—originated from the observation by Vogel and Risken [7] that the collection of probability distributions $\{p(x, \phi)\}$ for $\phi \in [0, \pi)$ is just the Radon transform—i.e. the *tomography*—of the Wigner function W . Therefore, by a Radon transform inversion, one can obtain W , and from W the matrix elements of the density operator ρ . This first method, however, was affected by uncontrollable approximations, since, as we will see in Subsect. 3’4, the inversion of the Radon transform needs an *analytic knowledge* of the probability distributions $p(x, \phi)$. In practice, the method works quite well for many photons and *quasi*-classical states, but fails when truly nonclassical states need to be determined experimentally. The main tool, however—i.e. using homodyning—still remains good: one only needs to avoid the intermediate step of determining W .

In Ref.[8] the first exact technique was given for measuring experimentally the matrix elements of ρ in the photon-number representation, by just averaging functions of homodyne data. After that, the method was further simplified [9], and the feasibility for

⁽¹⁾ One can adopt a Schrödinger-picture point of view, and instead of measuring varying operators one can vary the state itself in a controlled way, and eventually measure its energy[5]

nonunit quantum efficiency $\eta < 1$ at detectors—above some bounds—was established. Further improvements in the numerical algorithms made the method so simple and fast that it could be implemented easily on small PCs, and the method became quite popular in the laboratories (for the earlier progresses and improvements the reader can see the old review [10]). In the meanwhile there has been an explosion of interest on the subject of *measuring quantum states*, with hundreds of papers, both theoretical and experimental. The exact homodyne method has been implemented experimentally to measure the photon statistics of a semiconductor laser [11], and the density matrix of a squeezed vacuum [12]. The success of optical homodyne tomography has then stimulated the development of state reconstruction procedures for atomic beams [13], the experimental determination of the vibrational state of a molecule [14], of an ensemble of helium atoms [15], and of a single ion in a Paul trap [16], and different state reconstruction methods have been proposed (for an extensive list of references, see Ref. [17]).

In more recent years, the method of quantum tomography has been generalized to the estimation of an arbitrary observable of the field [18], with any number of modes [19], and, finally, to arbitrary quantum systems via group theory [20, 21, 22], and with a general method for unbiased noise [20, 21]. The use of maximum likelihood strategies [23] has made possible to reduce dramatically the number of experimental data (by a factor $10^3 \div 10^5$!) with negligible bias for most practical cases of interest. Finally, very recently, a method for tomographic estimation of the unknown quantum operation [24] of a quantum device has been presented [25], exploiting the “quantum parallelism” of an entangled input state which plays the role of a “superposition of all possible input states”. By another kind of quantum parallelism, one can also estimate the ensemble average of all operators of a quantum system by measuring only one fixed “universal” observable on an extended Hilbert space [26]—this is, in a sense, a sort of *Quantum Holography*. Eventually, after the last developments [27], now for first time we are in position of getting a first *theory* [28] that is based on the mathematical method of “frames” of operators. This theory will allow to classify all possible “quorums” of observables—i. e. those sets of observables that are sufficient to make a tomography of a given quantum system—and generally we will be able to answer to the question: “given a set of available measuring devices and transformation apparatuses, which ensemble averages can be estimated with them? Are they sufficient for a tomographic estimation?”

After briefly giving the general definition of what is quantum tomography in Sect. **2**, I will review the method of quantum homodyne tomography in Sect. **3**, with a brief introduction to balanced homodyne detection in Subsect. **3**’1. The first Radon transform approach is explained in Subsect. **3**’2, with the connection to the imaging procedure—which gave the name “tomography” to the method—in Subsect. **3**’3. The limitations of the Radon transform approach are explained in Subsect. **3**’4, and after, in Subsect. **3**’5 the exact tomographic approach is given, with the method for unbiased noise from nonunit quantum efficiency in Subsect. **3**’6. A very short account of the multimode homodyne tomography is given in Subsect. **3**’7, and improvements based on adaptive techniques and on the maximum likelihood strategy are rapidly introduced in Subsect. **3**’8, with some basic hints on how to estimate the ensemble averages of unbounded

operators in Subsect. 3'9. Most of the technical difficulties in homodyne tomography are due to the infinite dimension of the Hilbert space: for finite dimensions everything becomes particularly easy, as in the case of the Pauli tomography given in Sect. 4. With modern words from quantum information theory, we would regard homodyne tomography as the tomography of the so-called *continuous variables*, and the Pauli tomography as the tomography for *qubits*. Some experimental results from Ref. [34] on tomography of a twin-beam from parametric downconversion of vacuum are reported in Sect. 5. The general idea of how to perform tomography of a quantum device is explained in Sect. 6. Finally, Sect. 7 concludes the paper, with some basic hints and perspectives on a future general theory.

2. – Definition of the problem

Quantum Tomography is a method for estimating the ensemble average $\langle O \rangle$ of arbitrary operator O of a quantum system from measurements of a set—so-called *quorum*—of noncommuting observables. Obviously, the observables of the *quorum* are measured each at a time, with many repeated measurements on an ensemble of equally prepared quantum systems. In the practical situation we want the possibility of unbiased estimation from instrumental noise. Moreover, for concrete applications, we need to extend it to the estimation of the matrix of the "quantum operation" that describes the evolution in a device: this will really make quantum tomography a kind of *quantum radiography* of devices.

How can we make it? Let's first analyze the original method that originated from Ref. [7], and then see what we can really do better than that.

3. – Homodyne tomography, i.e. tomography for *continuous variables*

3'1. *The balanced homodyne detector.* – The balanced homodyne detector is certainly one of the most powerful experimental tools that we have in quantum optics. In fact, by the homodyne detector we can measure all quadratures $X_\phi = \frac{1}{2}(a^\dagger e^{i\phi} + a e^{-i\phi})$ of a field mode at any desired phase ϕ with respect to the local oscillator, which is equivalent to measuring all possible linear combinations of position and momentum of the field mode harmonic oscillator. This is a truly fortunate situation, which does not occur in the quantum mechanics of massive particles.

The basic scheme of the balanced homodyne detector is depicted in Fig. 1. The "signal" mode a is combined by means of a 50-50 beam splitter with a "local oscillator" (LO) mode b operating at the same frequency of a , and prepared in an "intense" coherent state $|z\rangle$. The signal mode a here plays the role of the "system of interest", whereas mode b has to be considered as a part of the apparatus. The field at the output of the beam splitter is described by a "sum" mode $c = (a + b)/\sqrt{2}$ and a "difference" mode $d = (a - b)/\sqrt{2}$. These output modes are detected by two identical photodetectors, and finally the difference of the photocurrents (at zero frequency) is rescaled by $2|z|$. Thus,

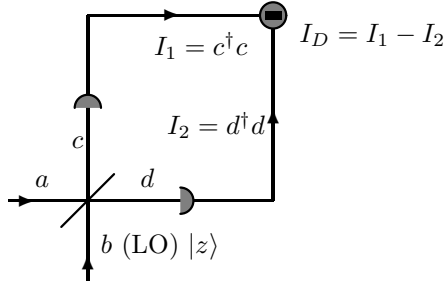


Fig. 1. – Basic scheme of a balanced homodyne detection.

the output of the detector is given by the following operator:

$$(1) \quad I_D = \frac{c^\dagger c - d^\dagger d}{2|z|} = \frac{a^\dagger b + b^\dagger a}{2|z|}.$$

From Eq. (1) we can immediately see that the expectation of the output I_D coincides with the expectation of the quadrature X_ϕ , with $\phi = \arg(z)$ being the tunable phase of the LO. Moreover, one can prove rigorously [10] that *in the strong-LO limit $z \rightarrow \infty$ the full probability distribution of the output current I_D approaches exactly the full probability distribution $p(x, \phi)$ of the quadrature X_ϕ , and this for any state ρ of the signal mode a .* In practice, we need $\langle a^\dagger a \rangle \ll |z|^2$, which is what we actually have in the real experiment. However, what we don't have in the laboratory is a couple of perfect photodetectors for the two modes c and d . On the other hand, since the input currents of the two detectors are both very intense, we can use in practice detectors that behave very linearly for intense inputs, without dark current, and with the only practical limitation that they have non perfect quantum efficiency, namely that they don't reveal all input photons. The fraction of actually revealed photons is called *quantum efficiency*, and is usually denoted by η . A detector that is sensitive to a very small number of photons—as an avalanche detector—not only saturates soon and exhibits dark current, but it also has very low quantum efficiency. On the contrary, for intense inputs we can easily find detectors that have really good quantum efficiencies, such as $\eta \simeq .9$ or better. A theoretical analysis based on the Mandel-Kelley-Kleiner formula [3] shows that in all respects a detector with quantum efficiency $\eta < 1$ is equivalent to an ideal detector preceded by a beam splitter with transmissivity η , and the output becomes a Bernoulli convolution of the response of an ideal detector. In the balanced homodyne detector with two identical detectors with $\eta < 1$, the output photocurrent is reduced by a factor η , and in order to measure the quadrature X_ϕ we now need to re-scale the photocurrent by $2|z|\eta$. Then, one can prove rigorously [3] that the probability distribution of the output photocurrent is just the Gaussian convolution of the ideal distribution, with rms $\Delta_\eta \equiv \sqrt{(1-\eta)/(4\eta)}$. In the actual case, further losses in the beam splitter will also reduce the overall effective η , and reasonable values that can be achieved are $\eta = .7 \div .8$.

3.2. Homodyne Tomography. – The first hint [7] on how to reconstruct the density matrix of a field mode from homodyne measurements originated from the simple fact that the collection of probability distributions $\{p(x, \phi)\}$ for variable phase $\phi \in [0, \pi)$ is just the Radon transform of the Wigner function $W(\alpha, \bar{\alpha})$, $\alpha \in \mathbb{C}$, namely

$$(2) \quad p(x, \phi) = \int_{-\infty}^{+\infty} dy W((x + iy)e^{i\phi}, (x - iy)e^{-i\phi}),$$

where the Wigner function is defined as usual as

$$(3) \quad W(\alpha, \bar{\alpha}) = \int \frac{d^2\lambda}{\pi^2} e^{\alpha\bar{\lambda} - \bar{\alpha}\lambda} \text{Tr}(\rho e^{\lambda a^\dagger - \bar{\lambda} a}).$$

Then, from the set of probability distributions $\{p(x, \phi)\}$ one can obtain the Wigner function by inversion of Eq. (2), namely

$$(4) \quad W(\alpha, \bar{\alpha}) = \int_{-\infty}^{+\infty} \frac{dk|k|}{4} \int_0^\pi \frac{d\phi}{\pi} \int_{-\infty}^{+\infty} dx p(x, \phi) \exp[ik(x - \alpha_\phi)],$$

where $\alpha_\phi = \Re(\alpha e^{-i\phi})$, and from the knowledge of $W(\alpha, \bar{\alpha})$ one can recover the matrix elements of the density operator ρ via the Fourier transform steps

$$(5) \quad \langle x + x' | \rho | x - x' \rangle = \int_{-\infty}^{\infty} dy e^{2ix'y} W(x + iy, x - iy),$$

$$(6) \quad \rho_{nm} = \sqrt{\frac{2^{1-n-m}}{\pi n! m!}} \int_{-\infty}^{\infty} dx \int_{-\infty}^{\infty} dx' e^{-(x^2 + x'^2)} H_n(\sqrt{2}x) H_m(\sqrt{2}x') \langle x | \rho | x' \rangle.$$

3.3. Why the name “tomography”? – The essential problem of tomographic imaging is to recover a distribution of mass in a 2-d slab from a finite collection of one dimen-

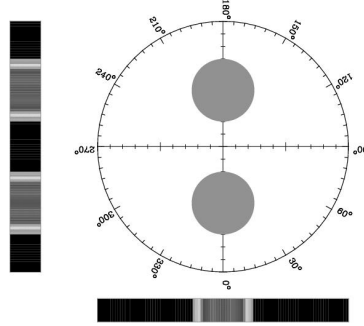


Fig. 2. – Illustration of the tomographic reconstruction of a 2-d image (here two holes in a uniform background) from its 1-d transmission profiles at different angles ϕ .

sional projections at different angles ϕ . The situation is schematically sketched in Fig. 2,

where the distribution of mass describes two circular holes in a uniform background. The tomographic machine—for example, an X-ray equipment—collects many stripe-photos of the sample from various directions ϕ , and then numerically performs a mathematical transform in order to reconstruct the density of mass from its radial profiles at different ϕ . The word “tomography” is customary to denote such imaging procedure starting from radial projections. The situation is strictly analogous to the inversion from the set of quadrature probability distributions $\{p(x, \phi)\}$ to the Wigner function $W(\alpha, \bar{\alpha})$, where now $p(x, \phi)$ plays the role of the radial projection at angle ϕ , and $W(\alpha, \bar{\alpha})$ is the density of mass on \mathbb{C} . The collection of all projections $\{p(x, \phi)\}$ at different ϕ 's is called *Radon transform*. The reconstruction of the “image” $W(\alpha, \bar{\alpha})$ from its “projections” $p(x, \phi)$ —this reconstruction is also called “back-projection”—is given by the inverse Radon transform (4).

3.4. Limitations of the Radon transform method . – Suppose that now you want to obtain the Wigner function as an average over ϕ and over homodyne outcomes. This means that in Eq. (4) the integral over k must be exchanged with those over ϕ and x , obtaining

$$(7) \quad W(\alpha, \bar{\alpha}) = \int_0^\pi \frac{d\phi}{\pi} \int_{-\infty}^{+\infty} dx p(x, \phi) \left[-\frac{1}{2} \text{P} \frac{1}{(x - \alpha_\phi)^2} \right],$$

$$(8) \quad \text{P} \frac{1}{z^2} \equiv \lim_{\varepsilon \rightarrow 0^+} \Re \frac{1}{(z + i\varepsilon)^2}, \quad \alpha_\phi = \Re(\alpha e^{-i\phi}),$$

P denoting the Cauchy principal value. Now $W(\alpha, \bar{\alpha})$ is the “expectation” (7) of an unbounded function over data distributed according to $p(x, \phi)$, with random phase ϕ . However, we cannot estimate the expectation as an average over experimental data, since the averaged function is unbounded, and does not satisfy the conditions for the central limit theorem. Averaging unbounded functions (non square summable) leads to results that never approach any definite value for large number of data, with rms errors that do not re-scale as as the inverse square root of the number of data. An example of this behaviour from computer simulated data is given in Fig. 3.

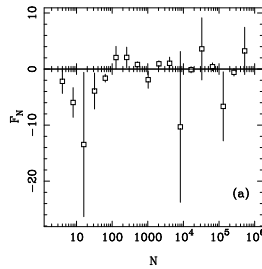


Fig. 3. – Numerical simulation of experiments for estimating the “average” of $f(x) = \frac{1}{x}$ with uniform probability $p(x) = 1/2$ for $x \in [-1, 1]$.

3'5. The exact method. – In the Radon transform method the Radon transform inversion is achieved by analytical approximations of the histograms of data and/or introducing a cut-off, for example the parameter ε in Eq. (8). The effect on the final matrix elements via Eqs. (5) and (6) is a bias, whose size depends on ρ and on the number of data. However, since the state ρ is unknown—we want to determine it!—we have now a logical loophole. Worst than that, we don't have any formula to bound the bias, and without any analytical control we cannot realize that, for example, there are bounds for quantum efficiency, as we will see in Subsect. 3'6.

The main idea at the basis of the exact method is that the unbounded kernel to be averaged is an artifact of passing through the Wigner function via the Radon transform inversion. Why then not bypass the evaluation of $W(\alpha, \bar{\alpha})$ and go directly to the matrix elements? As you will see soon, in this way not only one gets a method that has no approximation, but also one can recognize the route for generalizing the method to the estimation of any ensemble average for any quantum system. Before deriving the exact method we want to emphasize that for infinite-dimensional Hilbert spaces, as the one of the harmonic oscillator, an experimental knowledge of the density matrix elements ρ_{nm} doesn't necessarily provide an estimate of the ensemble average of any desired observable. In fact, if we try to obtain the ensemble average $\langle H \rangle$ of the operator H by summing the series $\langle H \rangle = \sum_{nm} \rho_{nm} H_{nm}$ with the matrix elements H_{nm} of H and the measured matrix elements ρ_{nm} of the state, we incur into the situation that even though the series for $\langle H \rangle$ converges in average, it may not converge in error! In fact, as we will see soon, the statistical errors $\varepsilon^2[\rho_{nm}]$ do not vanish for large n, m , and, as a result, for any finite number of data when we increase the series cut-off we ultimately get an unbounded error $\varepsilon^2[H] \simeq \sum_{nm} \varepsilon^2[\rho_{nm}] |H_{nm}|^2$. This is the case, for example, of the photon-number operator $H = a^\dagger a$. Again, we are repeating the same error of the inverse Radon transform method: we don't need to estimate the ensemble average of H via the matrix elements ρ_{nm} , but we can bypass the estimation of ρ_{nm} and directly evaluate a function whose average over data and over ϕ gives us the desired expectation value. Let's see now how this can be done.

The displacement operators $D(\alpha) = e^{\alpha a^\dagger - \alpha^* a}$ for $\alpha \in \mathbb{C}$ are an orthonormal basis (in the Dirac sense) for the Hilbert space of Hilbert-Schmidt operators, since $\text{Tr}[D^\dagger(\beta)D(\alpha)] = \pi\delta^{(2)}(\alpha - \beta)$. This means that we have the expansion

$$(9) \quad H = \int \frac{d^2\alpha}{\pi} \text{Tr}[HD(\alpha)] D^\dagger(\alpha).$$

By changing to polar variables: $\alpha = \frac{i}{2}k e^{i\phi}$ and using the symmetry $X_{\phi+\pi} = -X_\phi$ we can rewrite Eq. (9) as follows

$$(10) \quad H = \int_0^\pi \frac{d\phi}{\pi} \int_{-\infty}^{+\infty} \frac{dk|k|}{4} \text{Tr}[H e^{ikX_\phi}] e^{-ikX_\phi}.$$

By taking the ensemble average of both sides, and exchanging the integrals with the ensemble average, we can rewrite Eq. (10) as the double average of an *estimator* $E_H(X_\phi, \phi)$

over ϕ and over the ensemble

$$(11) \quad \langle H \rangle = \int_0^\pi \frac{d\phi}{\pi} \langle E_H(X_\phi, \phi) \rangle, \quad E_H(x, \phi) \doteq \int_{-\infty}^{+\infty} \frac{dk |k|}{4} \text{Tr}[H e^{ikX_\phi}] e^{-ikx}.$$

Notice that now, thanks to the trace with H , the last integral doesn't necessarily diverge as the one that gives the Cauchy principal value in Eq. (8). In a general theory[28] one classifies the operators H which gives a bounded trace in Eq. (11), and such that the integral over k converges. In the present simple form the method will need H at least Hilbert-Schmidt—which is the case of the outer product $|n\rangle\langle m|$ that gives the estimate of the matrix elements ρ_{nm} . However, as we will see in Subsect. 3'9, the method can be extended to a large class of unbounded operators. Anyway, just for the matrix elements ρ_{nm} , bypassing the step of the Wigner function has awarded us with a kernel that is now perfectly bounded, as we will see in the next subsection.

3'6. Unbiasing noise from nonunit quantum efficiency. – As we have seen in Subsection 3'1, the effect of nonunit quantum efficiency of the homodyne detector results in an additional Gaussian noise. This can be conveniently described as a completely positive (CP) map Γ_η , whose effect on the displacement operators is

$$\Gamma_\eta(\exp(ikX_\phi)) = \exp(ikX_\phi) e^{-\frac{1-\eta}{8\eta} k^2},$$

Now, we can “un-bias” the tomographic estimation by finding an new estimator $E_H^{(\eta)}(x, \phi)$ such that

$$(12) \quad \langle H \rangle = \int_0^\pi \frac{d\phi}{\pi} \langle E_H^{(\eta)}(X_\phi, \phi) \rangle_\eta,$$

where $\langle \dots \rangle_\eta$ denotes the *experimental* ensemble average, i. e. with the noisy state $\Gamma_\eta^\tau(\rho)$ — Γ_η^τ denoting the same noise map in the Schrödinger picture, i.e. the *dual* or *transposed* map. One has:

$$(13) \quad E_H^{(\eta)}(X_\phi, \phi) \doteq \Gamma_\eta^{-1} \{E_H(X_\phi)\} = \int_{-\infty}^{+\infty} \frac{dk |k|}{4} e^{\frac{1-\eta}{8\eta} k^2} \text{Tr}[H e^{ikX_\phi}] e^{-ikX_\phi}.$$

As an example, consider the case of the estimation of the matrix element $\rho_{n+d,n}$, i.e. $H = |n\rangle\langle n+d|$. The derivation of the estimator is the following

$$(14) \quad \begin{aligned} E_{|n\rangle\langle n+d|}^{(\eta)}(x, \phi) &= \int_{-\infty}^{\infty} \frac{dk |k|}{4} e^{-\frac{2\eta-1}{8\eta} k^2 - ikx} \langle n+d| : e^{ikX_\phi} : |n\rangle = \\ &= e^{id(\phi + \frac{\pi}{2})} \sqrt{\frac{n!}{(n+d)!}} \int_{-\infty}^{\infty} dk |k| e^{-\frac{2\eta-1}{2\eta} k^2 - i2kx} k^d L_n^d(k^2), \end{aligned}$$

where $: \dots :$ denotes normal ordering, and $L_n^d(x)$ are generalized Laguerre polynomials. Notice that the estimator is bounded only for $\eta > \eta_b = \frac{1}{2}$, and below this bound the

method would give unbounded statistical errors. However, as we have seen in Subsect. 3.1, this bound is well below the values that are reasonably achieved in the lab. Here I want to remind that a more efficient algorithm than the estimator in Eq. (14) is available, which uses factorization formulas that hold for $\eta = 1$ [29, 30], and then un-biases the noise from quantum efficiency via the inversion of the Bernoulli convolution, which obviously holds above the bound $\eta_b = \frac{1}{2}$ (see Ref. [10] for a concise review).

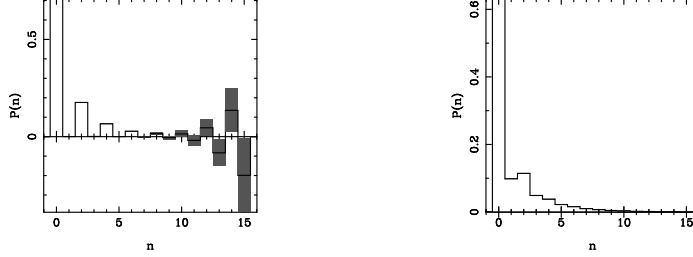


Fig. 4. – Tomographic reconstruction of the photon-number probability $P(n) \equiv \rho_{nn}$ of a squeezed vacuum ($\langle a^\dagger a \rangle = 1$) with detection efficiency $\eta = .8$. Homodyne data are computer simulated. (Here we averaged over 27 phases using 200 blocks of 5×10^5 data for each phase.) Experimental errors (confidence intervals) are represented by the gray-shaded thickness of horizontal lines. Left: unbiased reconstruction. Right: reconstruction without unbiasing. From Ref. [9].

An example of application of the estimator (14) to computer simulated data is given in Fig. 4 for the diagonal matrix element ρ_{nn} . There we can see that the price to be paid for the unbiasing procedure is to have statistical errors exponentially growing for increasingly large n . On the contrary, for $\eta = 1$ —with no need for unbiasing—the error would remain bonded for $n \rightarrow \infty$. In Ref. [31] the following asymptotic estimate of the statistical variance has been derived for $n \gg (2\eta - 1)/(1 - \eta)$ and $\eta < 1$:

$$(15) \quad \sigma^2[\rho_{n,n}] \simeq \frac{\eta^{3/2}}{\sqrt{\pi(1-\eta)n}} e^{\frac{1}{4n} \frac{(2\eta-1)^2}{\eta(1-\eta)}} \left(\frac{1}{2\eta-1} \right)^{2n+1},$$

whereas for $\eta = 1$ one simply has $\sigma^2[\rho_{n,n}] \simeq \sqrt{2}$. The mechanism that develops statistical errors is related to the oscillations of the estimator $E_{|n\rangle\langle n+d|}^{(\eta)}(x, \phi)$. In Fig. 5 we report some plots of the estimator $E_{|n\rangle\langle n+d|}^{(\eta)}(x, \phi)$ for different values of n, d and η . One can see that for $d = 0$ —along the diagonal of the matrix—the range of the kernel is bounded between -2 and 2 , and increases slowly versus the distance d from the diagonal. For increasing n and d the kernel oscillates fast, with an increasing number of nodes. Fast oscillations make the average of the kernel—hence the measured value ρ_{nm} —more sensitive to fluctuations of the quadrature outcomes x , producing confidence intervals that increase versus n and d . On the other hand, the bounded range makes errors themselves bounded, so they saturate at large n 's. For $\eta < 1$ the behavior of the kernel changes dramatically, with its range increasing versus n more and more fast as η approaches the lower bound $\eta = 0.5$.

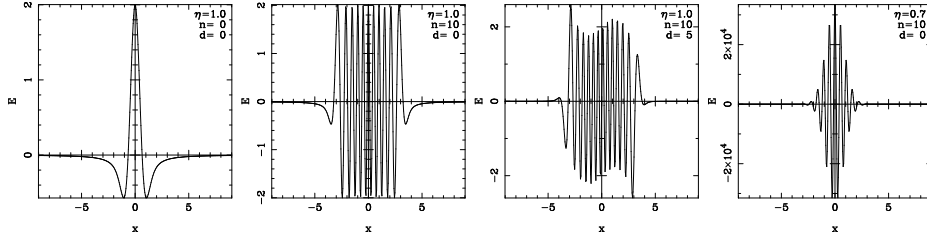


Fig. 5. – Estimator $E_{|n\rangle\langle n+d|}^{(\eta)}(x, \phi)$ of the matrix element $\rho_{n+d,n}$ for $\phi = 0$ and different values of n, d and η .

3.7. Multimode homodyne tomography. – For many radiation modes the method is easily generalized by using estimators for tensor product operators which are just the products of their relative estimators, i. e. for $M + 1$ modes one has $E_{\otimes_{n=0}^M O_n}^{(\eta)}(\{x_n\}, \{\phi_n\}) = \prod_{n=0}^M E_{O_n}^{(\eta)}(x_n, \phi_n)$. The case of a general operator is then obtained by linearity. However, this method needs a separate measurement—whence a separate LO—for each mode. In Ref. [19] it is shown that it is possible to estimate the expectation value of any multi-mode observable using a single LO, scanning all possible linear combinations of modes on the LO. For the derivation of the method the reader is addressed to Ref. [19]. Here we just report the final form of the estimator

$$(16) \quad E_O^{(\eta)}(x; \theta, \psi) = \frac{\kappa^{M+1}}{M!} \int_0^\infty dt e^{-t+2i\sqrt{\kappa}tx} t^M \text{Tr}\{O: \exp[-2i\sqrt{\kappa}tX(\theta, \psi)]:\},$$

where $: \dots :$ denotes normal ordering, $\kappa = \frac{2\eta}{2\eta-1}$, and the quadrature operator $X(\theta, \psi)$ is the following linear combination of single-mode quadratures

$$(17) \quad X(\theta, \psi) = \frac{1}{2} [A^\dagger(\theta, \psi) + A(\theta, \psi)], \quad A(\theta, \psi) = \sum_{l=0}^M e^{-i\psi_l} u_l(\theta) a_l,$$

a_l and a_l^\dagger ($l = 0, \dots, M$) being the annihilation and creation operators of the $M + 1$ independent modes with $[a_l, a_{l'}^\dagger] = \delta_{ll'}$, $\theta = (\theta_0, \dots, \theta_M)$ and $\psi = (\psi_0, \dots, \psi_M)$ denoting hyper-polar angles with ranges $\psi_l \in [0, 2\pi]$ and $\theta_l \in [0, \pi/2]$, whereas $u_l(\theta)$ are hyper-spherical coordinates, such that $\sum_{l=0}^M u_l^2(\theta) = 1$, with $u_0(\theta) = \cos \theta_1$, $u_1(\theta) = \sin \theta_1 \cos \theta_2$, $u_2(\theta) = \sin \theta_1 \sin \theta_2 \cos \theta_3$, \dots , $u_{M-1}(\theta) = \sin \theta_1 \sin \theta_2 \dots \sin \theta_{M-1} \cos \theta_M$, $u_M(\theta) = \sin \theta_1 \sin \theta_2 \dots \sin \theta_{M-1} \sin \theta_M$. The ensemble average $\langle O \rangle$ is obtained by averaging the estimator (16) as follows

$$(18) \quad \langle O \rangle = \int d\mu[\psi] \int d\mu[\theta] p(x, \theta, \psi) E_O^{(\eta)}(x, \theta, \psi),$$

where

$$(19) \quad \int d\mu[\psi] \doteq \prod_{l=0}^M \int_0^{2\pi} \frac{d\psi_l}{2\pi},$$

and

$$(20) \quad \int d\mu[\theta] \doteq 2^M M! \prod_{l=1}^M \int_0^{\pi/2} d\theta_l \sin^{2(M-l)+1} \theta_l \cos \theta_l.$$

In particular, one can estimate the matrix element $\langle \{n_l\} | R | \{m_l\} \rangle$ of the joint density matrix of modes. This will be obtained by averaging the following estimator

$$(21) \quad E_{|\{m_l\}\rangle\langle\{n_l\}|}^{(\eta)}(x, \theta, \psi) = e^{-i \sum_{l=0}^M (n_l - m_l) \psi_l} \frac{\kappa^{M+1}}{M!} \prod_{l=0}^M \left\{ [-i \sqrt{\kappa} u_l(\theta)]^{\mu_l - \nu_l} \sqrt{\frac{\nu_l!}{\mu_l!}} \right\} \\ \times \int_0^\infty dt e^{-t + 2i \sqrt{\kappa} t x} t^{M + \frac{1}{2}} \sum_{i=0}^M (\mu_i - \nu_i) \prod_{l=0}^M L_{\nu_l}^{\mu_l - \nu_l} [\kappa u_l^2(\theta) t],$$

where $\mu_l = \max(m_l, n_l)$, and $\nu_l = \min(m_l, n_l)$. In Fig. 6 we report some computer simulations from Ref. [19].

3.8. Improving statistical errors. – One of the major limitations of the unbiased tomographic methods are the quite large statistical errors. These, however, can be improved in several ways. One way of doing it is to exploit the non unicity of the estimators. As a matter of fact, there are “null estimators”, which have zero expectation for arbitrary probability $p_\eta(x, \phi)$, i. e. for arbitrary state ρ . Null estimators are obtained as linear combinations of the following functions[32]

$$(22) \quad N_{k,n}(X_\phi) = X_\phi^k e^{\pm i(k+2+2n)\phi} \quad k, n \geq 0.$$

The reader can easily check that they have zero average over ϕ , independently of ρ . Hence, for every operator O one actually has an equivalence class of infinitely many unbiased estimators, which differ by a linear combination of functions $N_{k,n}$. It is then possible to minimize the rms error in the equivalence class by the least-squares method, obtaining in this way an optimal estimator that is *adapted* to the particular set of experimental data. For details on this *adaptive techniques*, the reader is addressed to Ref. [32].

Another relevant strategy, the maximum likelihood method, can be used for measuring unknown parameters of a unitary transformation on a given state, or for measuring the matrix elements of the density operator itself [23]. For the full joint density matrix R of many modes, for example, the likelihood function would be

$$(23) \quad \mathcal{L} = \sum_i \log \left(\sum_{kn} |\langle \{n_i\} | T W_k^\dagger | \vec{x}_i \rangle_{\lambda_i}|^2 \right) - \beta \text{Tr}(T^\dagger T),$$

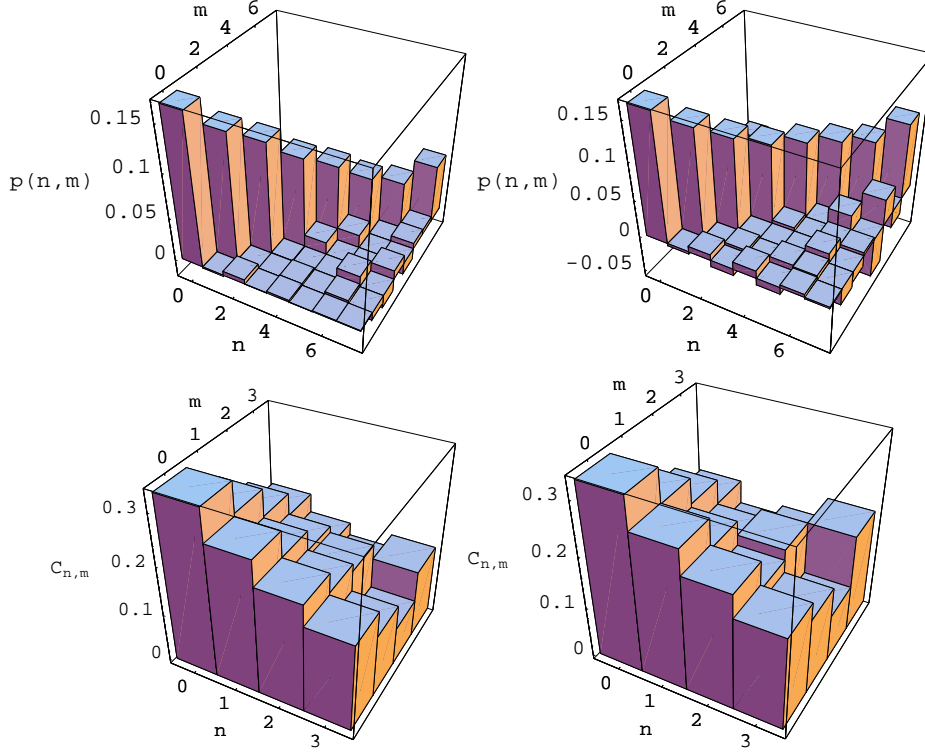


Fig. 6. – The two top figures show the two-mode photon-number probability $p(n, m)$ of the twin-beam state of parametric fluorescence for average number of photons per beam $\bar{n} = |\xi|^2/(1 - |\xi|^2) = 5$ obtained by a Monte Carlo simulation with random parameters $\cos 2\theta$, ψ_1 , and ψ_2 . The first figure is for quantum efficiency $\eta = 1$, and a sample of 10^6 data. The second figure is for quantum efficiency $\eta = .9$, and a sample of $5 * 10^6$ data. The two bottom figures show the tomographic reconstruction of the matrix elements $C_{n,m} \equiv {}_a \langle m|_b \langle m|\Psi\rangle \langle \Psi|n\rangle_a |n\rangle_b$ of the twin-beam state $|\Psi\rangle$ from parametric fluorescence for average number of photons per beam $\bar{n} = 2$. The first figure is for quantum efficiency $\eta = .9$, and a sample of 10^6 data, the second figure is for quantum efficiency $\eta = .8$, and a sample of $3 * 10^6$ data. From Ref. [19].

where β is a Lagrange multiplier, T is an upper triangular matrix in the Cholesky decomposition $R = T^\dagger T$ of the density matrix R , W_k —with $\sum_k W_k^\dagger W_k = I$ —are a Kraus decomposition $\Gamma[A] = \sum_k W_k^\dagger A W_k$ of the noise Γ (e. g. quantum efficiency), $\{|n_j\rangle\}$ denotes the photon-number basis, $|\vec{x}_i\rangle$ is the joint eigenvector of quadratures, and, finally, the sum runs over the label of the i th measurement. Notice that, since this method needs a finite parametrization of the density matrix, we need to truncate the Hilbert space dimension. However, much smaller statistical errors are obtained, as compared to the averaging procedure of Subsect. 3.6. An example of computer-simulated experiment is given in Fig. 7. We want to emphasize that the maximum likelihood method is not always the optimal solution of the tomographic problem, since it suffers from some major

limitations. Besides being biased due to the Hilbert space truncation—even though the bias can be very small if, from other methods, we know where to truncate—moreover it cannot be generalized to the estimation of any ensemble average, but just of a set of parameters from which ρ depends. In addition, for increasing number of modes the method has exponential complexity, since it requires a search of a maximum over all possible matrix elements. This should be compared with the procedure of Subsect. 3.7, which has polynomial (linear) complexity, and where we can estimate just one matrix element at the time. Therefore, the maximum likelihood strategy has to be regarded more as a complementary method of the unbiased averaging method. Finally, we want to notice that both the adaptive and the maximum likelihood improvements can be implemented for the general tomographic approach to arbitrary quantum system [21]: especially for the adaptive technique the general mathematical theory that uses operator frames [28] is]

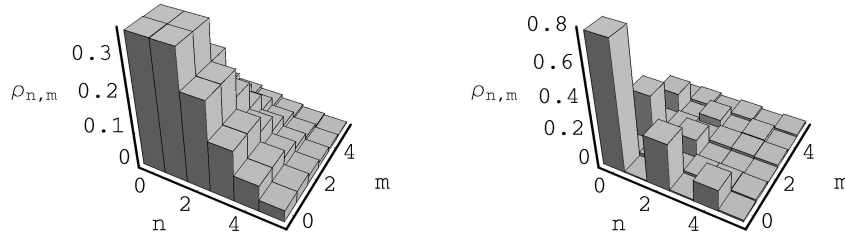


Fig. 7. – From Ref.[32]. Monte Carlo simulation of the tomographic reconstruction of the density matrix using the maximum likelihood technique. Left: density matrix for a coherent state with $\langle a^\dagger a \rangle = 1$; Right: squeezed vacuum with $\langle a^\dagger a \rangle = 0.5$. Both: 100 phases with 5000 data each. Hilbert space truncation set to $N_H = 5$; quantum efficiency $\eta = 0.8$.

3.9. Estimating ensemble averages of unbounded operators. – The estimator (11), which comes from the expansion (9) with displacement operators, cannot be used for estimating the ensemble average of operators which are not traceclass. However, one can easily recognize that, for example, an estimator for the field operator a is given by $E_a^{(\eta)}(X_\phi, \phi) = 2e^{i\phi} X_\phi$, and for the number operator easily one gets $E_{a^\dagger a}^{(\eta)}(X_\phi, \phi) = 2X_\phi^2 - \frac{1}{2\eta}$. By analytic methods Richter [33] has found the following estimators for normal ordered monomials in the field operators [then extended to $\eta < 1$ and s -ordering in Ref. [20]]:

$$(24) \quad E_{:a^\dagger m a^n:s}^{(\eta)}(X_\phi, \phi) = e^{i(n-m)\phi} \frac{H_{m+n} \left(\sqrt{\frac{2}{s_\eta}} X_\phi \right)}{\binom{n+m}{n} \left(\sqrt{2/s_\eta} \right)^{n+m}}, \quad s_\eta \doteq s - 1 + \eta^{-1}$$

where s is the usual ordering parameter ($s = 1$ for normal ordering, $s = -1$ for anti-normal ordering, $s = 0$ for symmetrical ordering), and $H_n(x)$ denote Hermite polynomials. From Eq. (24) one can recover a general expansion for a large class of unbounded operators, that here we report just for $\eta = 1$:

$$(25) \quad H = \int_0^\pi \frac{d\phi}{\pi} \int_{-\infty}^\infty dt \operatorname{Tr}[HG_{t,\phi}^\dagger] F_{t,\phi}, \quad F_{t,\phi} = \frac{1}{\sqrt{2\pi}} \exp[2(X_\phi + it/2)^2],$$

$$G_{t,\phi}^\dagger = \frac{d}{dt} t \int_0^1 d\theta \exp[\theta(1-\theta)t^2] e^{-ie^{i\phi}\theta ta^\dagger} |0\rangle\langle 0| e^{-ie^{-i\phi}(1-\theta)ta}.$$

A systematic method for finding estimators for unbounded operators is provided by the general theory based on operator frames [28], and is based on the idea of changing the definition of the scalar product in the operator expansion (see Sect. 7).

4. – Pauli Tomography, i.e. tomography for *qubits*

Most of the technical difficulties in homodyne tomography are due to the infinite dimension of the Hilbert space. For finite dimensions everything becomes particularly easy, since we can expand operators without concerns about convergence of the expansion. The easiest case is the two-state system—the *qubit*—for which the Pauli matrices with the identity $\{I, \sigma_x, \sigma_y, \sigma_z\}$ play the role of an orthonormal basis of observables. One has the following simple expansion

$$(26) \quad H = \frac{1}{2} \{ \vec{\sigma} \cdot \operatorname{Tr}[\vec{\sigma}H] + I \operatorname{Tr}[H] \}.$$

which gives the tomographic estimation

$$(27) \quad \langle H \rangle = \frac{1}{3} \sum_{\alpha=x,y,z} \langle E_H(\sigma_\alpha; \alpha) \rangle, \quad E_H(\sigma_\alpha; \alpha) = \frac{3}{2} \operatorname{Tr}[H\sigma_\alpha] \sigma_\alpha + \frac{1}{2} \operatorname{Tr}[H].$$

It is also very simple to unbiased the noise, by just inverting its CP map. For example, for a Pauli channel with $0 \leq p \leq 1$

$$(28) \quad \Gamma_p(H) = (1-p)H + \frac{p}{2} \operatorname{Tr}[H],$$

one has the unbiased estimator

$$(29) \quad E_H^{(p)}(\sigma_\alpha; \alpha) = \frac{3}{2(1-p)} \operatorname{Tr}[H\sigma_\alpha] \sigma_\alpha + \frac{1}{2} \operatorname{Tr}[H].$$

In quantum optics it is easy to implement a qubit using single photon polarized states, such as $|\uparrow\rangle \equiv |1\rangle_h |0\rangle_v$ and $|\downarrow\rangle \equiv |0\rangle_h |1\rangle_v$, where h and v denote horizontal and vertical polarization, respectively. The Pauli matrix σ_z is then given by the difference $\sigma_z = h^\dagger h - v^\dagger v$ of the horizontally and the vertically polarized photon-numbers, and can be measured

by means of a polarizing beam splitter as in Fig. 8. Similarly, it is easy to recognize that the other two Pauli matrices can be measured by the same scheme, preceded by a suitably oriented $\lambda/4$ plate, which transforms vertical-horizontal polarization to left-right circular polarization for σ_y , and to orthogonal linear diagonal polarizations for σ_x (see Fig. 8). This easily follows from the identities $\sigma_y = e^{i\frac{\pi}{4}\sigma_x}\sigma_z e^{-i\frac{\pi}{4}\sigma_x}$, which gives $e^{-i\frac{\pi}{4}\sigma_x}|1\rangle_h|0\rangle_v = \frac{1}{\sqrt{2}}[|1\rangle_h|0\rangle_v - i|0\rangle_h|1\rangle_v] \equiv |1\rangle_l|0\rangle_r$, and $\sigma_x = e^{-i\frac{\pi}{4}\sigma_y}\sigma_z e^{i\frac{\pi}{4}\sigma_y}$, which gives $e^{i\frac{\pi}{4}\sigma_y}|1\rangle_h|0\rangle_v = \frac{1}{\sqrt{2}}[|1\rangle_h|0\rangle_v - |0\rangle_h|1\rangle_v] \equiv |1\rangle_{\swarrow}|0\rangle_{\searrow}$.

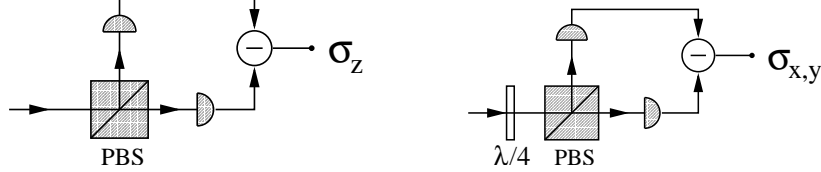


Fig. 8. – Pauli-matrix detectors for photon-polarization qubits (PBS=polarizing beam splitter).

5. – Some experimental results

We will not attempt to review the large experimental literature in quantum tomography: some references have been given in the introduction of this paper. Here we want to report some results from the experiment of Ref. [34]—in which the present author has been involved—since the same apparatus can be used for a homodyne tomography of a quantum device, as explained in Sect. 6. The experiment of Ref. [34] is actually the first measurement of the joint photon-number probability distribution for a two-mode quantum state created by a nondegenerate optical parametric amplifier. In this experiment, the two twin beams are detected separately by two balanced-homodyne detectors. A schematic of the experimental setup is reported in Fig. 9, and some experimental results are reported in Fig. 10. As expected for parametric fluorescence, the experiment has shown a measured joint photon-number probability distribution that exhibited up to 1.9 dB of quantum correlation between the two modes, with thermal marginal distributions.

6. – Tomography of a Quantum Device

What does mean performing the quantum tomography of a device? In quantum mechanics, the most general input-output evolution of a device—such as an amplifier, a measuring apparatus, etc.—is described by the state transformation

$$(30) \quad \rho \rightarrow \frac{\mathbf{E}(\rho)}{\text{Tr}(\mathbf{E}(\rho))},$$

which occurs with probability $p = \text{Tr}[\mathbf{E}(\rho)] \leq 1$. The *quantum operation* \mathbf{E} is a linear, trace-decreasing CP map.

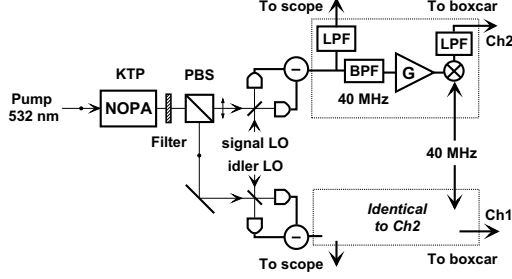


Fig. 9. – A schematic of the experimental setup. NOPA: non-degenerate optical parametric amplifier; LOs: local oscillators; PBS: polarizing beam splitter; LPFs: low-pass filters; BPF: band-pass filter; G: electronic amplifier. Electronics in the two channels are identical. From Ref. [34].

Suppose now that we have a quantum device that performs an unknown quantum operation E , and we want to determine it experimentally. How can we do? We can exploit the one-to-one correspondence $E \leftrightarrow R_E$ between quantum operations and positive operators R_E on two copies of the Hilbert space $\mathbf{H} \otimes \mathbf{H}$, which is given by

$$(31) \quad R_E = E \otimes \mathbf{I}_{\mathbf{H}}(|I\rangle\rangle\langle\langle I|), \quad E(\rho) = \text{Tr}_2[I \otimes \rho^\tau R_E],$$

where for an operator $O = \sum_{nm} O_{nm}|n\rangle\langle m|$ the notation O^τ means the transposed operator $O^\tau = \sum_{nm} O_{mn}|n\rangle\langle m|$ with respect to some pre-chosen orthonormal basis $\{|n\rangle\}$. In the following we will use the notation $|A\rangle\rangle \doteq \sum_{nm} A_{nm}|n\rangle \otimes |m\rangle \equiv A \otimes I|I\rangle\rangle \equiv I \otimes A^\tau|I\rangle\rangle$ that exploits the isomorphism between the Hilbert space of the Hilbert-Schmidt operators $A, B \in \text{HS}(\mathbf{H})$ with scalar product $\langle\langle A, B \rangle\rangle \doteq \text{Tr}[A^\dagger B]$ and the Hilbert space of bipartite vectors $|A\rangle\rangle, |B\rangle\rangle \in \mathbf{H} \otimes \mathbf{H}$, where one has $\langle\langle A|B \rangle\rangle \equiv \langle\langle A, B \rangle\rangle$. If we consider an entangled input state $|\psi\rangle\rangle$ and operate with E only on one party of $|\psi\rangle\rangle$, as in Fig. 11, the output state is the joint density matrix

$$(32) \quad |\psi\rangle\rangle\langle\langle\psi| \rightarrow R(\psi) \equiv E \otimes \mathbf{I}(|\psi\rangle\rangle\langle\langle\psi|).$$

But now the quantum operation E is in correspondence with $R_E \equiv R(\psi)$ for $\psi = I$, and for invertible ψ the two matrices $R(I)$ and $R(\psi)$ are connected as follows

$$(33) \quad R(I) = (I \otimes \psi^{-1\tau})R(\psi)(I \otimes \psi^{-1*}),$$

where $O^* = \sum_{nm} O_{nm}^*|n\rangle\langle m|$ denotes the conjugate operator of $O = \sum_{nm} O_{nm}|n\rangle\langle m|$. Hence, the quantum operation (four-index) matrix R_E can be obtained by estimating via a joint double quantum tomography the following output ensemble averages

$$(34) \quad \langle\langle i, j|R(I)|l, k \rangle\rangle = \left\langle |l\rangle\langle i| \otimes |\psi^{-1*}(k)\rangle\langle\psi^{-1*}(j)| \right\rangle,$$

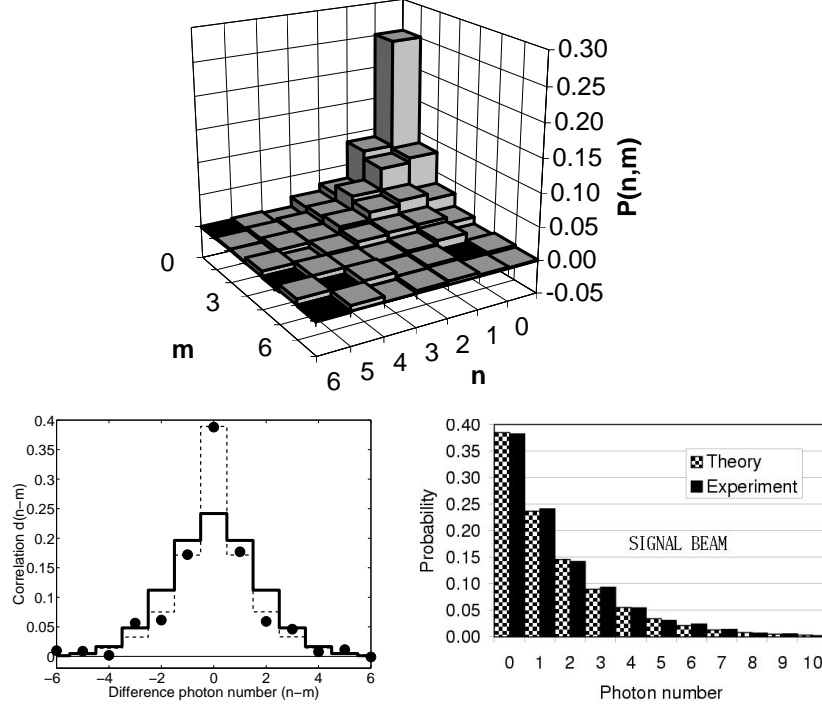


Fig. 10. – Top: Measured joint photon-number probability distributions for the twin-beam state. Bottom left: Difference photon-number distributions corresponding to the left graphs. Filled circles: experimental data; solid lines: theoretical predictions; dashed lines, difference photon-number distributions for two independent coherent states with the same total mean number of photons and $\bar{n} = \bar{m}$. 400000 samples, $\bar{n} = \bar{m} = 1.5$, $N = 10$. Bottom right: Marginal distributions for the signal beam for the same data. Theoretical distributions for the same mean photon numbers are also shown. Very similar results are obtained for the idler beam. From Ref. [34].

where $|v^*\rangle$ denotes the conjugate vector $|v^*\rangle = \sum_n v_n^* |n\rangle$ of $|v\rangle = \sum_n v_n |n\rangle$.

In Fig. 12 the results from a homodyne tomography of an optical displacement of one of the two twin beams from parametric downconversion of the vacuum are reported from Ref. [25] for a simulated experiment, for displacement parameter $z = 1$, and for some typical values of the quantum efficiency η at homodyne detectors and of the mean thermal photon number \bar{n} of the twin beams. As one can see a meaningful reconstruction of the matrix can be achieved in the given range with $10^6 \div 10^7$ data, but this number can be decreased of a factor 100–1000 using the tomographic maximum likelihood techniques of Subsect. (3·8), however, at the expense of the complexity of the algorithm. Homodyne quantum efficiencies and amplifier gains (for the twin beams) typical of the experimental setup of Ref. [34] are considered. Improving quantum efficiency and increasing the amplifier gain (toward a maximally entangled state) have the effect of making statistical

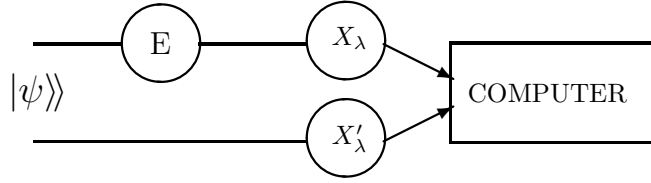


Fig. 11. – General experimental scheme of the method for the tomographic estimation of a quantum operation. Two identical quantum systems are prepared in an entangled state $|\psi\rangle\rangle$. One of the two systems undergoes the quantum operation E , whereas the other is left untouched. At the output one makes a quantum tomographic estimation, by measuring jointly two observables X_λ and X'_λ from two quorums $\{X_\lambda\}$ and $\{X'_\lambda\}$ of observables for the two Hilbert spaces, such as two different quadratures of the two field modes in a two-mode homodyne tomography.

errors smaller and more uniform versus the photon labels n and m of the matrix A_{nm} . Meaningful reconstructions can be achieved with as few as $\bar{n} \sim 1$ thermal photons, and with quantum efficiency as low as $\eta = 0.7$.

7. – Conclusions and future perspectives

What is quantum tomography in general, in simple words? As a method to estimate the ensemble average $\langle H \rangle$ of any arbitrary operator H on a Hilbert space \mathbb{H} by using only measurement outcomes of a *quorum* of observables $\{O(l)\}$, it must be essentially a technique for expanding operators over a set of functions $f_n(O(l))$ of the observables

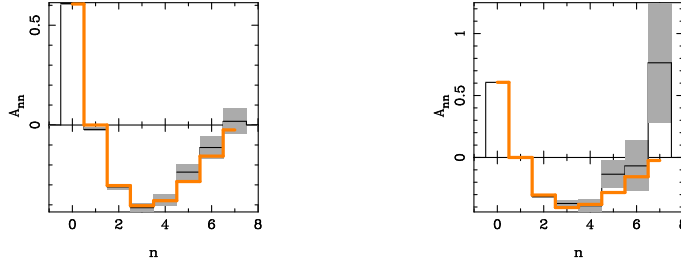


Fig. 12. – From Ref.[25]. Homodyne tomography of the quantum operation corresponding to the unitary displacement of one mode of the radiation field. Diagonal elements D_{nn} of the displacement operator (shown by thin solid line on an extended abscissa range), with their respective error bars in gray shade, compared to the theoretical probability (thick solid line). Similar results are obtained for all upper and lower diagonals of the quantum operation matrix A . The reconstruction has been achieved using an entangled state $|\psi\rangle\rangle$ at the input corresponding to parametric downconversion of vacuum with mean thermal photon \bar{n} and quantum efficiency at homodyne detectors η . Left: $z = 1$, $\bar{n} = 5$, $\eta = 0.9$, and 150 blocks of 10^4 data have been used. Right: $z = 1$, $\bar{n} = 3$, $\eta = 0.7$, and 300 blocks of $2 \cdot 10^5$ data have been used. The plot on the right corresponds to the same parameters of the experiment in Ref. [34].

$\{O(l)\}$. What makes a general theory nontrivial is the fact that the set of observables $\{O(l)\}$ generally does not span the operator space, whereas it is the set of operators $f_n(O(l))$ —*nonlinear* in $\{O(l)\}$ —that is complete for varying n and l . Let's denote by $P(j)$ such complete set of operators. Once you have the $P(j)$, then the problem is reduced to the *linear* problem of expanding an operator as $H = \sum_j \langle Q^\dagger(j), H \rangle P(j)$, for a suitable “dual” set of operators $\{Q(j)\}$. Now the point is to have a scalar product $\langle A, B \rangle$ in the expansion that is not just the Hilbert-Schmidt $\langle A, B \rangle \equiv \text{Tr}[A^\dagger B]$, since we want to expand also operators that are not Hilbert-Schmidt. This can be done by changing the definition of the scalar product. The mathematical *theory of frames* [35, 36] is the perfect tool for establishing completeness and for finding dual sets $\{Q(j)\}$. Notice that in most practical situations, the non orthogonal set $\{P(j)\}$ is over-complete, and there are many alternate dual sets $\{Q(j)\}$: such non unicity is the basis for general adaptive techniques. Finally, I want to emphasize that a general theory should also classify the operators H which have bounded scalar product with $\{Q(l)\}$ and bounded expansion $H = \sum_j \langle Q^\dagger(j), H \rangle P(j)$, and also assess how these classes are restricted when a noise is unbiased. Only in this way one would be able to say which ensemble averages can be actually estimated and which noise can be unbiased. For the reader that is interested in these future developments, I suggest to look on the Los Alamos ArXive for the forthcoming manuscript [28].

REFERENCES

- [1] FANO U., *Rev. Mod. Phys.*, **29** (1957) 74.
- [2] PAULI W., *Encyclopedia of Physics*, (S) pringer, Berlin) 1958, Vol. V, p. 17.
- [3] D'ARIANO G. M., *Quantum Estimation Theory and Optical Detection*, in *Concepts and Advances in Quantum Optics and Spectroscopy of Solids*, edited by BY T. HAKIOĞLU and A. S. SHUMOVSKY (Kluwer Academic Publishers, Amsterdam) 1997, pp. 139-174.
- [4] D'ESPAGNAT B., *Conceptual Foundations of Quantum Mechanics* (W. A. Benjamin, Mass.), 1976.
- [5] ROYER A., *Found. Phys.*, **19** (1989) 3
- [6] SMITHEY D. T., BECK M., RAYMER M. G. and FARIDANI A., *Phys. Rev. Lett.*, **70** (1993) 1244.
- [7] VOGEL K. and RISKEN H., *Phys. Rev. A*, **40** (1989) 2847.
- [8] D'ARIANO G. M., MACCHIAVELLO C. and PARIS M. G. A., *Phys. Rev. A*, **50** (1994) 4298.
- [9] D'ARIANO G. M., LEONHARDT U. and PAUL H., *Phys. Rev. A*, **52** (1995) R1801.
- [10] D'ARIANO G. M., *Measuring Quantum States*, in the same book of Ref. [3], pp. 175-202.
- [11] MUNROE M., BOGGAVARAPU D., ANDERSON , M. E. and RAYMER M. G., *Phys. Rev. A*, **52** (1995) R924
- [12] SCHILLER S., BREITENBACH G., PEREIRA S. F., MÜLLER T. and MLYNEK J., *Phys. Rev. Lett.*, **77** (1996) 2933; BREITENBACH G., SCHILLER S. and MLYNEK J., *Nature*, **387** (1997) 471.
- [13] JANICKE U. and WILKENS M., *J. Mod. Opt.*, **42** (1995) 2183; WALLENTOWITZ S. and VOGEL W., *Phys. Rev. Lett.*, **75** (1995) 2932; KIENLE S. H., FREIBERGER M., SCHLEICH W. P. and RAYMER M. G., in *Experimental Metaphysics: Quantum Mechanical Studies for Abner Shimony* ed. by S. COHEN ET AL. (Kluwer, Lancaster) 1997, p. 121.
- [14] DUNN T. J., WALMSLEY I. A. and MUKAMEL S., *Phys. Rev. Lett.*, **74** (1995) 884.
- [15] KURTSIEFER C., PFAU T. and MLYNEK J., *Nature* **386**, **1997** (150)

- [16] LEIBFRIED D., MEEKHOF D. M., KING B. E., MONROE C., ITANO W. M. and WINELAND D. J., *Phys. Rev. Lett.*, **77** (1996) 4281
- [17] D'ARIANO G. M., VASILYEV M. and KUMAR P., *Phys. Rev. A*, **58** (1998) 636
- [18] D'ARIANO G. M., *Homodyning as universal detection*, in *Quantum Communication, Computing, and Measurement*, edited by O. HIROTA, A. S. HOLEVO and C. M. CAVES (Plenum Publishing, New York and London), 1997, p. 253.
- [19] D'ARIANO G. M., KUMAR P. and SACCHI M., *Phys. Rev. A*, **61** (2000) 13806.
- [20] D'ARIANO G. M., *Latest developments in quantum tomography*, in *Quantum Communication, Computing, and Measurement*, edited by P. KUMAR, G. M. D'ARIANO and O. HIROTA (Kluwer Academic/Plenum Publishers, New York and London), 2000, p. 137.
- [21] D'ARIANO G. M., *Phys. Lett. A*, **268** (2000) 151.
- [22] CASSINELLI G., D'ARIANO G. M., DE VITO E. and LEVRERO A., *J. Math. Phys.*, **41** (2000) 7940.
- [23] BANASZEK K., D'ARIANO G. M., PARIS M. G. A. and SACCHI M., *Phys. Rev. A*, **61** (2000) 010304.
- [24] KRAUS K., *States, Effects, and Operations* (Springer-Verlag, Berlin), 1983.
- [25] D'ARIANO G. M. and LO PRESTI P., *Phys. Rev. Lett.*, **86** (2001) 4195.
- [26] D'ARIANO G. M., *Phys. Lett. A* **300** 1 (2002)
- [27] D'ARIANO G. M., MACCONE L. and PARIS M. G. A., *J. Phys. A*, **34** (2001) 34; *Phys. Lett. A*, **276** (2000) 25.
- [28] D'ARIANO G. M., To appear on LANL arXive quant-ph/
- [29] RICHTER T., *Phys. Lett. A*, **221** (1996) 327
- [30] LEONHARDT U., MUNROE M., KISS T., RAYMER M. G. and RICHTER T., *Opt. Commun*, **127** (1996) 144
- [31] D'ARIANO G. M., MACCHIAVELLO C. and STERPI N. A., *Quantum Semiclass. Opt.*, **9** (1997) 929
- [32] D'ARIANO G. M. and PARIS M. G. A., *Phys. Rev. A*, **60** (1999) 518
- [33] RICHTER T., *Phys. Rev. A*, **53** (1996) 1197
- [34] VASILYEV M., CHOI S.-K., KUMAR P. and D'ARIANO G. M., *Phys. Rev. Lett.*, **84** (2000) 2354.
- [35] CASAZZA P, *Taiwanese J. Math.*, **4** (2000) 129
- [36] HAN D. and LARSON D. R., *Mem. Amer. Math. Soc.*, **147** (2000) n. 697 0-94 (AMS, Providence, Rhode Island)